arXiv:2209.12236v1 [quant-ph] 25 Sep 2022

Suppressing the decoherence of alkali-metal spins at low magnetic fields

Mark Dikopoltsev,[1,2,*] Avraham Berrebi,[1] Uriel Levy,[1] and Or Katz[3,4,†]

[1] *Department of Applied Physics, The Faculty of Science, The Center for Nanoscience and Nanotechnology, The Hebrew University of Jerusalem, Jerusalem 9190401, Israel.*
[2] *Rafael Ltd, 31021, Haifa, Israel.*
[3] *Duke Quantum Center, Duke University, Durham, NC 27701*
[4] *Department of Electrical and Computer Engineering, Duke University, Durham, NC 27708*

(Dated: September 27, 2022)

Interactions of electron spins with rotational degrees of freedom during collisions or with external fields are fundamental processes that limit the coherence time of spin gases. We experimentally study the decoherence of warm cesium spins dominated by spin rotation-interaction during binary collisions with N_2 molecules or by absorption of near-resonant light. We report an order of magnitude suppression of the spin decoherence rate by either of those processes at low magnetic fields. We find that the excess decoherence at higher magnetic fields originates from an asynchronous Larmor precession, which is a mechanism that universally affects all alkali atoms, and can yet be suppressed at low magnetic-fields. This work extends the widely-used regime of Spin-Exchange Relaxation Free (SERF), which provides protection from decoherence by random spin-conservative processes, now for random processes which do not conserve but rather destruct electron spins.

Ensembles of alkali-metal spins are a prominent physical system. They feature strong coupling to optical and magnetic fields and can be isolated from the environment for considerably long times at or above room-temperature. Therefore, they have wide-spread and evolving applications in quantum sensing and precision magnetometery [1–8], in searches of new physics [9–16], in interfacing and polarizing spins of noble-gases for imaging and fundamental studies [17–22], in coupling to opto-mechanical systems [23–25], in quantum information applications [26–35] and recently also in studies of new phases of matter [36].

The great coupling of the electron spin to external fields also sets the limit for which the spin state can be isolated from the environment before relaxing, affecting the performance of the aforementioned applications. The prominent relaxation mechanisms of alkali-metal spins originate from processes which couple predominantly to the valence electron spin, during collisions, by the action of external fields, or at the walls of the enclosure that holds the gas [37]. The latter can be suppressed by introducing buffer gas, typically mixtures of noble-gas atoms or diatomic molecules. This gas renders the motion diffusive and slows-down the collision rate of alkali-metal atoms with the glass walls [38]. However, buffer gas also acts to relax the alkali-metal's spin by the spin-rotation interaction, which couples the electron spin to the rotational angular momentum during collisions [38–41]. Other relxation mechanisms are associated with the action of external fields. For instance, optical fields tuned near the atomic transitions which are used, e.g. to dispersively probe the spin state of the alkali atoms, can be absorbed by the atoms and alter or relax their spin state [26, 29, 42].

The rate in which different relaxation mechanisms practically affect alkali-metal spins depends on the magnetic field orientation, which determines the quantization axis. Spins oriented along the field have a characteristic "longitudinal" spin-lifetime T_1 [37, 43, 44]. Spins that are oriented transverse to the field, have a coherence-time T_2 which is typically much shorter than the spin-lifetime for dense alkali-metal vapor. The reduced coherence time partially originates from processes such as random spin-exchange collisions between pairs of alkali-metal atoms, which predominantly decohere the spins but weakly affect their lifetime [37, 38, 45]. Nevertheless, decoherence due to random *spin-preserving* collisions can be usefully suppressed via control over the magnetic field magnitude in the μG-G range; It is utilized to suppress the decoherence caused by the random spin-exchange collisions and to drive the vapor into the Spin-Exchange Relaxation Free (SERF) regime [45–51]. Yet, the direct effect of the magnetic field magnitude on decoherence by processes which do not conserve the spins, such as spin-rotation interaction in collisions with buffer gas or absorption of light, has not been investigated below hundreds of Gauss [52–54].

Here we study decoherence that originates from processes that do not conserve the spin, and its dependence on the applied magnetic field. We report an order of magnitude suppression of the decoherence rate by the spin-rotation interaction during collisions of cesium vapor with N_2 molecules, and further show that the suppression is robust for a wide range of densities and degrees of spin-polarization. We additionally study the decoherence rate by absorption of near-resonant light and find an order of magnitude suppression at low magnetic fields. We present a simple model that identifies

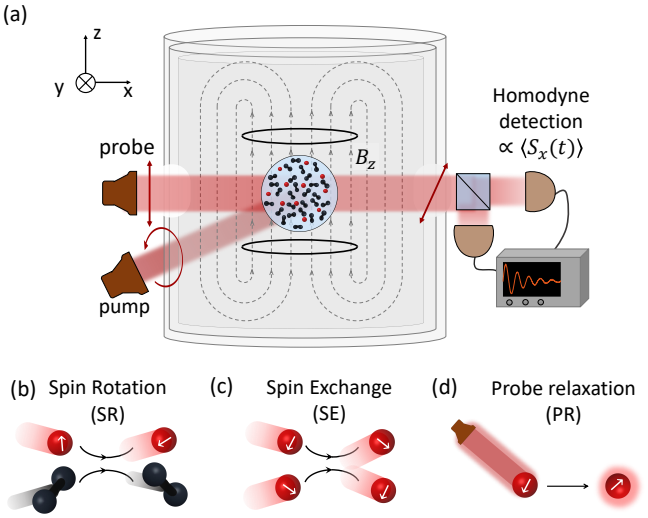


Figure 1. **Relaxation mechanisms and experimental apparatus.** (a) Cesium spins (red spheres) are enclosed with a dense molecular N_2 gas (black spheres) inside a spherical glass cell. The cesium spins are initially polarized by a short pulse of optical pumping, and subsequently start precessing around an applied magnetic field B_z. The spin evolution and coherence time is observed using an optical probe beam, which measures the average spin $\langle S_x(t)\rangle$ transverse to the magnetic field. (b-d) Processes which effect the electron spins' coherence time. (b) Randomization of the cesium's electron spin by the spin-rotation interaction during collisions with an N_2 molecule. (c) Exchange of electronic spins-between pairs of alkali metal atoms in collisions. (d) Absorption of near-resonance light which excites the cesium's electron and alters the spin state in the electronic ground-state after de-excitation. Unlike process (c) which instantaneously conserves the total spin of the colliding spins, processes (b) and (d) do not conserve but rather randomize the spin of the electron.

the origin of the decoherence in the presence of the magnetic field and its suppression at low magnetic-fields. This study can be directly applied in alkali-metal vapor based applications and experiments.

We experimentally study the decoherence of cesium vapor with N_2 gas using the apparatus in Fig. 1. The atoms are enclosed in a 1" diameter spherical glass cell, which contains 2.4 amagat of N_2 gas and a small cesium-metal droplet whose temperature determines the vapor number-density. The temperature is controlled using a home-made oven to maintain a constant cesium vapor pressure, and the cell is magnetically shielded using several layers of magnetic shields. We characterize the relaxation mechanisms by monitoring the dynamics of the cesium spins absent the pumping beam. We first optically pump the spins along a magnetic field in the xy plane using a circularly polarized beam that is tuned on resonance with the D_1 optical transition. The latter, appears as a single spectral line with a linewidth of about 40 GHz owing to pressure broadening by the N_2 gas. Then, we turn off these fields and apply a magnetic field $B\hat{z}$ which leads to Larmor precession. The average collective evolution of the alkali spins $\langle S_x(t)\rangle$ is monitored via measurement of the polarization rotation of a weak, far-detuned and linearly polarized optical probe beam in a homodyne configuration, which negligibly affects the evolution. Further details on the experimental configuration are provided in [55].

We measure the decoherence of the alkali metal spins $\langle S_x(t)\rangle$ as a function of the applied magnetic field $B\hat{z}$. At each value of the field, we fit the data to a simple model $\langle S_x(t)\rangle = Ae^{-t/T_2}\sin(\omega t+\phi)$ using A, ϕ, ω and T_2 as fitting parameters and t to denote time of evolution. In Fig. 2 we present the measured coherence time T_2 as a function of the applied magnetic field $B\hat{z}$ (blue circles). We observe a $\xi = 12$ fold suppression of the decoherence rate of the spins at low magnetic fields ($|B| \lesssim 0.04$ mG) with respect to the decoherence at moderate magnetic fields ($|B| \gtrsim 0.8$ mG). These results show that the spins' decoherence rate can be suppressed by more than an order of magnitude at low magnetic fields.

To compare the contribution of the spin-rotation interaction to all other relaxation processes, and ensure it is the dominant relaxation mechanism, we estimate the different relaxation rates in our experiment as detailed in [55], and summarized in Table I under the "SR exp." column. Via measurement of the cesium number density $n_{\mathrm{Cs}} = (3.3\pm0.3)\times10^{11}\,\mathrm{cm}^{-3}$, we estimate the various spin-relaxation rates affecting the valence electron; The rate $R_{\mathrm{sr}}^{(\mathrm{N_2})}$ by collisions of cesium and N_2, the spin-exchange rate R_{se} due to collisions between pairs of alkali-metal atoms and the spin-destruction rate R_{pr} by the weak probe beam. We also estimate and damping rate of the slowest diffusion mode R_{diff} by diffusion and destruction at the enclosure walls. These estimations agree well with the independently measured longitudinal spin lifetime $T_1 = (15.0\pm0.5)$ ms. Evidently, the spin-rotation rate $R_{\mathrm{sr}}^{(\mathrm{N_2})}$ highlighted in blue is the dominant relaxation mechanism of the vapor, surpassing all other rates by about an order of magnitude. We therefore conclude that the suppressed decoherence observed in Fig. 2 is associated predominantly with the spin-rotation interaction.

We also study the suppression for different degrees of spin polarization and to different cesium number densities. The initial spin polarization $P = T_1/(T_{\mathrm{pump}}+T_1)$ depends on the longitudinal optical-pumping time T_{pump} which we control and independently measure [55]. We estimate an initial spin polarization of $P = 0.15$ for the aforementioned experiment, which corresponds to the low-polarization limit. We repeat the experiment also for higher initial polarization $P = 0.66$ and find

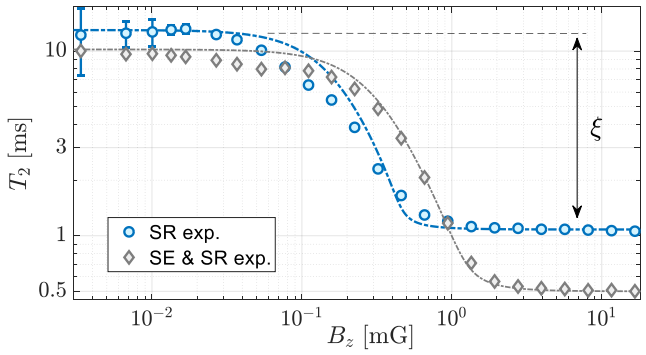


Figure 2. **Suppression of decoherence by spin-rotation.** The measured coherence time T_2 at low magnetic fields is prolonged by the suppression factor ξ with respect to high magnetic fields. We present two different configurations: lower vapor density (blue) where the suppression factor $\xi = 12$ is predominantly associated with the spin-rotation relaxation, and higher vapor density (grey) where $\xi = 20$ is associated with both the spin-rotation and spin-exchange which have comparable rates. The rates characterizing the two configurations are summarized in Table I under the columns SR and SE & SR, and the dashed lines correspond to the calculated relaxation rates as modeled in [55].

Rate $[2\pi \times \text{kHz}]$	SR exp.	SE & SR exp.	PR exp.
$R_{\text{sr}}^{(\text{N}_2)}$	1.9 ± 0.4	2.0 ± 0.4	1.9 ± 0.4
R_{se}	0.22 ± 0.02	5.3 ± 0.6	0.23 ± 0.02
R_{pr}	0.08 ± 0.03	0.14 ± 0.06	$30 \pm 2^{(*)}$
R_{wall}	< 0.001	< 0.001	< 0.001

Table I. **Relaxation rates for the three experimental configurations.** $R_{\text{sr}}^{(\text{N}_2)}$ denotes the relaxation rate of the electron spin by collisions with N_2 molecules, R_{se} denotes the spin exchange rate, R_{pr} is the relaxation by of the electron spin due to light absorption of the probe beam. In the column PR this value was achieved from spin relaxation time at the first millisecond of the decay process under powerful probe beam. And R_{wall} is the relaxation rate of the first diffusion mode by diffusion and interaction with the walls. The column SR corresponds to a configuration with low vapor density and low probe power, where the spin-rotation rate is dominant. The column SE & SR corresponds to a configuration with higher vapor density, where the rates of spin-rotation and spin-exchange are comparable. The coherence time of these two configuration is shown in Fig. 2 in blue and grey respectively. The column PR corresponds to low vapor density but high and near resonance optical probe beam, which renders the probe induced relaxation dominant. The evolution in the latter configuration is shown in Fig. 3. Calculation of all rates is detailed in [55]

similar behaviour and suppression factor ξ [55]. We also characterize the suppression at an elevated number density $n_{\text{Cs}} = (7.5 \pm 0.5) \times 10^{12}\,\text{cm}^{-3}$, in a configuration whose parameters appear under the "SE & SR exp." column in table I. Here the spin-exchange and spin-rotation rates are comparable, and their total measured decoherence, presented in in Fig. 2 (grey), is simultaneously suppressed at low magnetic fields. Frequent spin-exchange collisions also extend the range of usable magnetic fields for which the decoherence is maximally suppressed. These measurements demonstrate that the suppression of spin-rotation decoherence is robust for various degrees of spin polarization and alkali number densities, and that at low magnetic fields, the coherence time T_2 can be prolonged towards the spin-lifetime T_1.

We further study the spin-decoherence induced by absorption of near-resonant light. We repeat the experimental sequence for the parameters of "SR exp." but increase the optical power of the probe and tune its frequency near resonance with the optical D_1 transition. Consequently, the relaxation by the probe light R_{pr} is considerably increased and dominates the spins relaxation. We also increase the pump power in the preparation stage to set the initial polarization $P = 0.15$ despite the decreased lifetime $T_1 = 1.0 \pm 0.06$ msec. In Fig. 3 we present the short-time evolution of the mean spin component $\langle S_x(t) \rangle$ at three different magnetic fields. Evidently, the decoherence at low magnetic field is suppressed with respect to higher magnetic fields, and approaches spin-lifetime T_1. Owing to the Gaussian intensity profile of the probe and the slow diffusion of the atoms, the decay is multi-exponential [37, 38, 56] which precludes quantitative characterization by a single relaxation rate. Nonetheless, both the ratio of the linewidth of the signals in the frequency domain at high and low magnetic fields ($\xi = 19$) as well as the ratio between the $1/e$ time ($\xi = 28$) indicate that the decoherence is suppressed by more than an order of magnitude.

To elucidate the suppression mechanism for decoherence by processes which do not conserve the spins, we use a simple model which highlights the roles of the hyperfine interaction, the electron-relaxation process, and magnetic field precession in the low polarization limit. In alkali-metal atoms, the strong hyperfine interaction couples the electron spin S and the nuclear spin I, rendering the total spin $F = I + S$ and its projection along the magnetic field M to good quantum numbers. The relaxation mechanisms we consider here are coined as S-damping processes with relaxation rate R_{sd} [38], as they couple and effect predominantly the electron spin S owing to their short correlation time with respect to the hyperfine rate. Spin-rotation occurs during short and uncorrelated binary collisions of alkali-metal and buffer-gas pairs, each lasting a few picoseconds [38, 57]. For

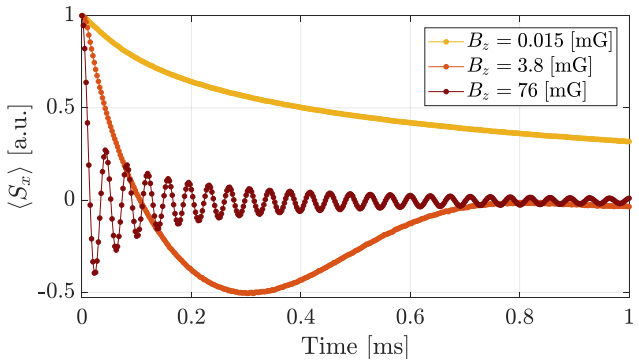


Figure 3. **Suppression of decoherence by optical absorption.** The transverse spin relaxes rapidly at high magnetic fields, but the relaxation is suppressed at low magnetic fields. In this configuration the probe power is increased and tuned near resonance to render its relaxation dominant (see the experimental parameters in Table I under the PR exp. coulmn). The measured decay is multi-exponential owing to the Gaussian shape of the probe beam [55].

the pressure-broadened optical transition in the experiment, the correlation time of both absorption of photons and of non-radiative de-excitation is associated with the inverse of the optical linewidth, corresponding to a few picoseconds.

As the relaxation mechanisms act to relax S but leave I intact, the latter acts as a flywheel: it partially stores the total spin orientation during a collision and repolarizes the electron spin afterwards. For spins oriented along the field, this mechanism is known to prolong the spin-lifetime T_1 by a factor q, known as the slowing-down factor, in comparison with the decay of an equivalent electron spin (i.e. $I = 0$) [37]. The fraction $1/q$ represents the fraction of angular momentum that is carried by the electron spin out of the total alkali-metal spin, and is lost in a collision. This fraction depends on the magnitude of the nuclear spin and the state of the ensemble, and can be cast via I, P and $R_{\rm sd}/R_{\rm se}$, as studied in Refs. [37, 45, 47] at different regimes. While spin-exchange collisions conserve the average vapor spin during the collision, at longer time scales they can effect the observed lifetimes by changing the spin population at the hyperfine manifolds while driving the system to follow a spin-temperature distribution. For cesium ($I = 7/2$) in the low polarization limit, the slowing-down factor is considerable: it ranges from $q = 22$ for rapid spin-exchange ($R_{\rm se} \gg R_{\rm sd}$) up to $q = 32$ when the destruction is dominant ($R_{\rm sd} \gg R_{\rm se}$).

The introduction of magnetic field however can hamper the flywheel mechanism for spins that are oriented perpendicular to the field. To capture this effect, we describe the evolution under magnetic field $B\hat{z}$ and S-damping collisions at rate $R_{\rm sd}$ using the simplified Bloch equations for infrequent spin-exchange collisions

$$\partial_t \langle F_+ \rangle = -\left(i g_e B + R_{\rm sd}\right) \langle S_+ \rangle \,, \tag{1}$$

$$\partial_t \langle S_+ \rangle = -i \frac{g_e B}{2q} \langle F_+ \rangle - R_{\rm sd}(\langle S_+ \rangle - \tfrac{1}{q} \langle I_+ \rangle). \tag{2}$$

Here $\langle F_+ \rangle = \langle F_x \rangle + i \langle F_y \rangle$ denotes the average total transverse spin of an alkali-metal atom and $\langle S_+ \rangle = \langle S_x \rangle + i \langle S_y \rangle$ denotes the average transverse spin of the electron. Eq. (1) describes the precession of the total spin induced by the Larmor precession of the electron spin where g_e is the electron gyromagnetic-ratio, as well as the decay due to damping of the electron spin at a rate $R_{\rm sd}$. The first term in Eq. (2) describes the back-action of the total spin on the electron which slows down its motion, the second term describes its damping, and the last term describes the flywheel repolarization by a fraction $q = (2I+1)^2/2$ via the transverse nuclear spin $\langle I_+ \rangle = \langle F_+ \rangle - \langle S_+ \rangle$.

Equations. (1-2) form a coupled set of two linear differential equations whose dynamics is characterized by the evolution of two modes; the imaginary part of the eigenvalues represent to the precession rates ω and the real part of the eigenvalues represent the decoherence rates T_2^{-1}. At high magnetic fields ($gB \gg R_{\rm sd}$) we find two precession rates $\omega = \pm g_e B/(2I+1)$ and two rapid decoherence rates are $T_2^{-1} = R_{\rm sd}(q \pm \sqrt{2q}+1)/(2q)$ that are associated with two modes: one in which the electron and nuclear spins are anti-aligned, and another in which they are aligned. These two modes correspond to the lower and upper hyperfine manifolds respectively, which precess at equal rates but with opposite directions. Owing to this sign difference, the Larmor precession of the different hyperfine manifolds which is initially in phase, becomes asynchronous and results with rapid decoherence of the ensemble-averaged signal. For $I \gg 1$, the coherence time of the two hyperfine manifolds approaches the same value of $T_2 \approx 2/R_{\rm sd}$, manifesting a rapid decay of the electron and nuclear spins and no re-polarization by the nucleus.

At low magnetic fields ($gB \ll R_{\rm sd}$) in contrast, the evolution of the nuclear and electron spins is highly correlated and the total spin is dominated by a single eigenvalue; Its over-damped precession rate is $\omega = g_e B/(2q-2)$ and its coherence time is $T_2 = q/R_{\rm sd}$. The ratio between the average coherence times in the low and high magnetic field regimes give the suppression factor $\xi \approx (I+\frac{1}{2})^2$, which is about $\xi \approx 16$ for cesium. This factor manifests the excess decoherence that originates from the asynchronous precession, and that can be suppressed at low magnetic fields for processes that do not conserve the electron spin.

To quantitatively compare the theoretical model with the experimental result, we cast the former in the standard form of the hyperfine-Bloch equations [58, 59], and

include also the spin-exchange term, as well as the small contribution of diffusion-damping [55]. The modeled response is shown in Fig. 2 (dot-dashed lines), and is in good agreement with the measured data.

In conclusion, we have experimentally demonstrated an order of magnitude suppression of T_2-type decoherence at low magnetic fields for processes that do not preserve the spin such as spin-rotation interaction and absorption of light. A simple model reveals that the suppression is owed to preservation of the nuclear spin of the alkali at low magnetic field, which is lost at moderate magnetic fields by uncorrelated Larmor precession of the magnetic moments in the two hyperfine manifolds. This work extends the use of magnetic-field as a tool to suppress decoherence that originates from processes which do not preserve the spins.

It is intriguing that the decoherence rates observed at moderate-high magnetic fields due to spin-destruction collisions or by absorption of light are only partially owing to the loss of spin during the collision. Instead, it is the coherent but asynchronous precession of the magnetic moments in the two hyperfine manifolds that dephases the average spin of the ensemble after few collisions. In the limit $I \gg 1$, the fraction of the total spin that is lost during a collision is so small that the dynamics and dephasing become akin to that of spin-exchange collisions where the relaxation of the uniform spin mode is only due to the asynchronous precession after redistribution of the spin population between the two hyperfine manifolds.

It is also interesting to consider the potential suppression of decoherence by other relaxation processes. The relaxation mechanisms we considered here coupled predominantly through the spin of the electron, owing to the short correlation time of the interaction. Other relaxation processes also have sizeable coupling to the electron spins. These processes include relaxation by spin-axis in collisions of alkali-metal pairs [43, 54], relaxation by the walls of anti-relaxation coated cells [60], and relaxation by very short-lived Van-der-Waals molecules [61]. It is therefore plausible that the decoherence rate by these processes would also be suppressed at lower magnetic fields.

* mark.dikopoltsev@mail.huji.ac.il
† or.katz@duke.edu

[1] D. Budker and M. Romalis, Optical magnetometry, Nature physics **3**, 227 (2007).
[2] I. Kominis, T. Kornack, J. Allred, and M. V. Romalis, A subfemtotesla multichannel atomic magnetometer, Nature **422**, 596 (2003).
[3] H. Dang, A. C. Maloof, and M. V. Romalis, Ultrahigh sensitivity magnetic field and magnetization measurements with an atomic magnetometer, Applied Physics Letters **97**, 151110 (2010).
[4] M. Balabas, D. Budker, J. Kitching, P. Schwindt, and J. Stalnaker, Magnetometry with millimeter-scale antirelaxation-coated alkali-metal vapor cells, JOSA B **23**, 1001 (2006).
[5] T. G. Walker and M. S. Larsen, Spin-exchange-pumped nmr gyros, in *Advances in atomic, molecular, and optical physics*, Vol. 65 (Elsevier, 2016) pp. 373–401.
[6] M. Ledbetter, I. Savukov, V. Acosta, D. Budker, and M. Romalis, Spin-exchange-relaxation-free magnetometry with cs vapor, Physical Review A **77**, 033408 (2008).
[7] S. Xu, V. V. Yashchuk, M. H. Donaldson, S. M. Rochester, D. Budker, and A. Pines, Magnetic resonance imaging with an optical atomic magnetometer, Proceedings of the National Academy of Sciences **103**, 12668 (2006).
[8] T. Theis, P. Ganssle, G. Kervern, S. Knappe, J. Kitching, M. Ledbetter, D. Budker, and A. Pines, Parahydrogen-enhanced zero-field nuclear magnetic resonance, Nature Physics **7**, 571 (2011).
[9] M. Jiang, H. Su, A. Garcon, X. Peng, and D. Budker, Search for axion-like dark matter with spin-based amplifiers, Nature Physics **17**, 1402 (2021).
[10] I. M. Bloch, Y. Hochberg, E. Kuflik, and T. Volansky, Axion-like relics: new constraints from old comagnetometer data, Journal of High Energy Physics **2020**, 1 (2020).
[11] I. M. Bloch, G. Ronen, R. Shaham, O. Katz, T. Volansky, and O. Katz, New constraints on axion-like dark matter using a floquet quantum detector, Science advances **8**, eabl8919 (2022).
[12] G. Vasilakis, J. Brown, T. Kornack, and M. Romalis, Limits on new long range nuclear spin-dependent forces set with a k- he 3 comagnetometer, Physical review letters **103**, 261801 (2009).
[13] D. Budker, P. W. Graham, M. Ledbetter, S. Rajendran, and A. O. Sushkov, Proposal for a cosmic axion spin precession experiment (casper), Physical Review X **4**, 021030 (2014).
[14] M. Safronova, D. Budker, D. DeMille, D. F. J. Kimball, A. Derevianko, and C. W. Clark, Search for new physics with atoms and molecules, Reviews of Modern Physics **90**, 025008 (2018).
[15] D. Budker, T. Cecil, T. E. Chupp, A. A. Geraci, D. F. J. Kimball, S. Kolkowitz, S. Rajendran, J. T. Singh, and A. O. Sushkov, Quantum sensors for high precision measurements of spin-dependent interactions, arXiv preprint arXiv:2203.09488 (2022).
[16] S. Afach, B. C. Buchler, D. Budker, C. Dailey, A. Derevianko, V. Dumont, N. L. Figueroa, I. Gerhardt, Z. D. Grujić, H. Guo, *et al.*, Search for topological defect dark matter with a global network of optical magnetometers, Nature Physics **17**, 1396 (2021).
[17] T. G. Walker and W. Happer, Spin-exchange optical pumping of noble-gas nuclei, Reviews of modern physics **69**, 629 (1997).
[18] T. R. Gentile, P. Nacher, B. Saam, and T. Walker, Optically polarized he 3, Reviews of modern physics **89**, 045004 (2017).
[19] R. Shaham, O. Katz, and O. Firstenberg, Strong cou-

pling of alkali-metal spins to noble-gas spins with an hour-long coherence time, Nature Physics **18**, 506 (2022).
[20] O. Katz, R. Shaham, and O. Firstenberg, Coupling light to a nuclear spin gas with a two-photon linewidth of five millihertz, Science advances **7**, eabe9164 (2021).
[21] T. Chupp and S. Swanson, Medical imaging with laser-polarized noble gases, in *Advances in Atomic, Molecular, and Optical Physics*, Vol. 45 (Elsevier, 2001) pp. 41–98.
[22] K. Coulter, A. McDonald, W. Happer, T. Chupp, and M. E. Wagshul, Neutron polarization with polarized 3he, Nuclear Instruments and Methods in Physics Research Section A: Accelerators, Spectrometers, Detectors and Associated Equipment **270**, 90 (1988).
[23] C. B. Møller, R. A. Thomas, G. Vasilakis, E. Zeuthen, Y. Tsaturyan, M. Balabas, K. Jensen, A. Schliesser, K. Hammerer, and E. S. Polzik, Quantum back-action-evading measurement of motion in a negative mass reference frame, Nature **547**, 191 (2017).
[24] R. A. Thomas, M. Parniak, C. Østfeldt, C. B. Møller, C. Bærentsen, Y. Tsaturyan, A. Schliesser, J. Appel, E. Zeuthen, and E. S. Polzik, Entanglement between distant macroscopic mechanical and spin systems, Nature Physics **17**, 228 (2021).
[25] F. Y. Khalili and E. S. Polzik, Overcoming the standard quantum limit in gravitational wave detectors using spin systems with a negative effective mass, Physical review letters **121**, 031101 (2018).
[26] K. Hammerer, A. S. Sørensen, and E. S. Polzik, Quantum interface between light and atomic ensembles, Reviews of Modern Physics **82**, 1041 (2010).
[27] H. Bao, J. Duan, S. Jin, X. Lu, P. Li, W. Qu, M. Wang, I. Novikova, E. E. Mikhailov, K.-F. Zhao, *et al.*, Spin squeezing of 1011 atoms by prediction and retrodiction measurements, Nature **581**, 159 (2020).
[28] O. Katz, R. Shaham, E. S. Polzik, and O. Firstenberg, Long-lived entanglement generation of nuclear spins using coherent light, Physical Review Letters **124**, 043602 (2020).
[29] J. Kong, R. Jiménez-Martínez, C. Troullinou, V. G. Lucivero, G. Tóth, and M. W. Mitchell, Measurement-induced, spatially-extended entanglement in a hot, strongly-interacting atomic system, Nature communications **11**, 1 (2020).
[30] O. Katz and O. Firstenberg, Light storage for one second in room-temperature alkali vapor, Nature communications **9**, 1 (2018).
[31] M. Hosseini, B. M. Sparkes, G. Campbell, P. K. Lam, and B. C. Buchler, High efficiency coherent optical memory with warm rubidium vapour, Nature communications **2**, 1 (2011).
[32] V. Guarrera, R. Gartman, G. Bevilacqua, and W. Chalupczak, Spin-noise spectroscopy of a noise-squeezed atomic state, Physical Review Research **3**, L032015 (2021).
[33] K. Mouloudakis, G. Vasilakis, V. Lucivero, J. Kong, I. Kominis, and M. Mitchell, Effects of spin-exchange collisions on the fluctuation spectra of hot alkali vapors, arXiv preprint arXiv:2204.08748 (2022).
[34] G. Buser, R. Mottola, B. Cotting, J. Wolters, and P. Treutlein, Single-photon storage in a ground-state vapor cell quantum memory, arXiv preprint arXiv:2204.12389 (2022).
[35] B. Julsgaard, A. Kozhekin, and E. S. Polzik, Experimental long-lived entanglement of two macroscopic objects, Nature **413**, 400 (2001).
[36] Y. Horowicz, O. Katz, O. Raz, and O. Firstenberg, Critical dynamics and phase transition of a strongly interacting warm spin gas, Proceedings of the National Academy of Sciences **118**, e2106400118 (2021).
[37] S. Appelt, A. B.-A. Baranga, C. Erickson, M. Romalis, A. Young, and W. Happer, Theory of spin-exchange optical pumping of 3 he and 129 xe, Physical review A **58**, 1412 (1998).
[38] Y.-Y. Jau, T. Walker, and W. Happer, *Optically pumped atoms* (John Wiley & Sons, 2010).
[39] Z. Wu, T. Walker, and W. Happer, Spin-rotation interaction of noble-gas alkali-metal atom pairs, Physical review letters **54**, 1921 (1985).
[40] T. G. Walker, Estimates of spin-exchange parameters for alkali-metal–noble-gas pairs, Physical Review A **40**, 4959 (1989).
[41] T. G. Walker, J. H. Thywissen, and W. Happer, Spin-rotation interaction of alkali-metal–he-atom pairs, Physical Review A **56**, 2090 (1997).
[42] K. Hammerer, K. Mølmer, E. S. Polzik, and J. I. Cirac, Light-matter quantum interface, Physical Review A **70**, 044304 (2004).
[43] S. Kadlecek, L. Anderson, C. Erickson, and T. Walker, Spin relaxation in alkali-metal 1 σ g+ dimers, Physical Review A **64**, 052717 (2001).
[44] M. T. Graf, D. F. Kimball, S. M. Rochester, K. Kerner, C. Wong, D. Budker, E. Alexandrov, M. Balabas, and V. Yashchuk, Relaxation of atomic polarization in paraffin-coated cesium vapor cells, Physical Review A **72**, 023401 (2005).
[45] W. Happer and A. Tam, Effect of rapid spin exchange on the magnetic-resonance spectrum of alkali vapors, Physical Review A **16**, 1877 (1977).
[46] W. Happer and H. Tang, Spin-exchange shift and narrowing of magnetic resonance lines in optically pumped alkali vapors, Physical Review Letters **31**, 273 (1973).
[47] I. Savukov and M. Romalis, Effects of spin-exchange collisions in a high-density alkali-metal vapor in low magnetic fields, Physical Review A **71**, 023405 (2005).
[48] A. Korver, R. Wyllie, B. Lancor, and T. Walker, Suppression of spin-exchange relaxation using pulsed parametric resonance, Physical review letters **111**, 043002 (2013).
[49] O. Katz, M. Dikopoltsev, O. Peleg, M. Shuker, J. Steinhauer, and N. Katz, Nonlinear elimination of spin-exchange relaxation of high magnetic moments, Physical review letters **110**, 263004 (2013).
[50] W. Chalupczak, P. Josephs-Franks, B. Patton, and S. Pustelny, Spin-exchange narrowing of the atomic ground-state resonances, Physical Review A **90**, 042509 (2014).
[51] R. Gartman, V. Guarrera, G. Bevilacqua, and W. Chalupczak, Linear and nonlinear coherent coupling in a bell-bloom magnetometer, Physical Review A **98**, 061401 (2018).
[52] D. Walter, W. Griffith, and W. Happer, Magnetic slowing down of spin relaxation due to binary collisions of

alkali-metal atoms with buffer-gas atoms, Physical review letters **88**, 093004 (2002).
[53] S. Kadlecek, L. Anderson, and T. Walker, Field dependence of spin relaxation in a dense rb vapor, Physical review letters **80**, 5512 (1998).
[54] C. Erickson, D. Levron, W. Happer, S. Kadlecek, B. Chann, L. Anderson, and T. Walker, Spin relaxation resonances due to the spin-axis interaction in dense rubidium and cesium vapor, Physical review letters **85**, 4237 (2000).
[55] See Supplemental Material at [URL inserted by publisher] for further details on the experimental setup, estimation of rates, the dependence of the decoherence on spin polarization, effective decoherence estimation by a non-uniform probe beam and the full hyperfine-Bloch equations.
[56] R. Shaham, O. Katz, and O. Firstenberg, Quantum dynamics of collective spin states in a thermal gas, Physical Review A **102**, 012822 (2020).
[57] W. Happer and W. Van Wijngaarden, An optical pumping primer, Hyperfine Interactions **38**, 435 (1987).
[58] W. Xiao, T. Wu, X. Peng, and H. Guo, Atomic spin-exchange collisions in magnetic fields, Physical Review A **103**, 043116 (2021).
[59] O. Katz, O. Peleg, and O. Firstenberg, Coherent coupling of alkali atoms by random collisions, Physical Review Letters **115**, 113003 (2015).
[60] M. Balabas, T. Karaulanov, M. Ledbetter, and D. Budker, Polarized alkali-metal vapor with minute-long transverse spin-relaxation time, Physical review letters **105**, 070801 (2010).
[61] I. Nelson and T. Walker, Rb-xe spin relaxation in dilute xe mixtures, Physical Review A **65**, 012712 (2001).